ARTICLE
Journal of Cellular Biochemistry 116:2008–2017 (2015)

Journal of Cellular Biochemistry

Regulation of *CYBB* Gene Expression in Human Phagocytes by a Distant Upstream NF-κB Binding Site

Josias B. Frazão,[1] Alison Thain,[2] Zhiqing Zhu,[2] Marcos Luengo,[3] Antonio Condino-Neto,[1] and Peter E. Newburger[2*]

[1]*Department of Immunology, Institute of Biomedical Sciences, University of São Paulo, São Paulo, SP 05508-900, Brazil*

[2]*Departments of Pediatrics and of Molecular, Cellular, and Cancer Biology, University of Massachusetts Medical School, Worcester, Massachusetts 01655*

[3]*Center for Investigation in Pediatrics, State University of Campinas Medical School, Campinas, SP 13081-970, Brazil*

ABSTRACT

The human *CYBB* gene encodes the gp91-*phox* component of the phagocyte oxidase enzyme complex, which is responsible for generating superoxide and other downstream reactive oxygen species essential to microbial killing. In the present study, we have identified by sequence analysis a putative NF-κB binding site in a DNase I hypersensitive site, termed HS-II, located in the distant 5′ flanking region of the *CYBB* gene. Electrophoretic mobility assays showed binding of the sequence element by recombinant NF-κB protein p50 and by proteins in nuclear extract from the HL-60 myeloid leukemia cell line corresponding to p50 and to p50/p65 heterodimers. Chromatin immunoprecipitation demonstrated NF-κB binding to the site in intact HL-60 cells. Chromosome conformation capture (3C) assays demonstrated physical interaction between the NF-κB binding site and the *CYBB* promoter region. Inhibition of NF-κB activity by salicylate reduced *CYBB* expression in peripheral blood neutrophils and differentiated U937 monocytic leukemia cells. U937 cells transfected with a mutant inhibitor of κB "super-repressor" showed markedly diminished *CYBB* expression. Luciferase reporter analysis of the NF-κB site linked to the *CYBB* 5′ flanking promoter region revealed enhanced expression, augmented by treatment with interferon-γ. These studies indicate a role for this distant, 15 kb upstream, binding site in NF-κB regulation of the *CYBB* gene, an essential component of phagocyte-mediated host defense. J. Cell. Biochem. 116: 2008–2017, 2015.

KEY WORDS: NF-κB; *CYBB*; PHAGOCYTE OXIDASE; ENHANCER; GENE EXPRESSION

Professional phagocytes, such as granulocytes and macrophages, contain a membrane-associated NADPH oxidase that generates superoxide [Nauseef and Borregaard, 2014]. This reactive oxygen species and its derivatives mediate many of the microbicidal, tumoricidal, and inflammatory activities of these cells [de Oliveira-Junior et al., 2011]. The catalytic subunit of the phagocyte oxidase enzyme complex is a membrane-spanning flavocytochrome *b* composed of a 91 kDa glycoprotein, termed gp91-*phox*, and a 22 kDa non-glycosylated polypeptide, termed p22-*phox*, encoded respectively by the *CYBB* and *CYBA* genes [Karimi et al., 2014; Nauseef and Borregaard, 2014]. Defects in these genes are responsible for the X-linked and one of the autosomal recessive forms of chronic granulomatous disease (CGD), a primary immunodeficiency disorder characterized by severe, recurrent bacterial and fungal infections [Roos and de Boer, 2014].

In hematopoietic cells, *CYBB* expression is limited to the granulocyte, monocyte/macrophage, and dendritic cell lineages during the process of terminal differentiation [Nauseef and Borregaard, 2014]. Phagocyte *CYBB* expression is tightly restricted to terminally differentiating myeloid cells that are beyond the promyelocyte stage [Nauseef and Borregaard, 2014], and is responsive to a number of inflammatory cytokines and stimuli

Josias B. Frazão and Alison Thain contributed equally to the work.

Grant sponsor: NIH; Grant number: DK-54369; Grant sponsor: FAPESP (Fundação de Amparo à Pesquisa do Estado de São Paulo); Grant numbers: 06/52483-1, 01/14365-3.

*Correspondence to: Peter E. Newburger, MD, University of Massachusetts Medical School, 55 Lake Avenue North, Worcester, MA 01605. E-mail peter.newburger@umassmed.edu

Manuscript Received: 2 March 2015; Manuscript Accepted: 3 March 2015

Accepted manuscript online in Wiley Online Library (wileyonlinelibrary.com): 9 March 2015

DOI 10.1002/jcb.25155 • © 2015 Wiley Periodicals, Inc.

such as IFN-γ, LPS, and TNF-α [Newburger et al., 1991; Gauss et al., 2007].

The proximal promoter region (−450 to +12 bp) of the *CYBB* gene is sufficient to provide transcriptional regulation of the gene in stably transfected myeloid cell lines [Eklund et al., 1996]. This promoter element contains binding sites for both functionally important repressors and enhancers of transcription. Multiple binding sites for the transcriptional repressor CCAAT displacement protein mediate restriction of gene expression to mature myeloid cells in cooperation with the nuclear matrix attachment region-binding protein SATB1 [Hawkins et al., 2001]. One of the CCAAT displacement protein recognition sites also binds the transcriptionally repressive homeobox protein HoxA10, which disengages upon tyrosine phosphorylation of the HoxA10 component during IFN-γ-induced differentiation in myeloid cells, leading to its release and replacement by the transcriptional activator HoxA9 [Bei et al., 2007].

Removal of these repressor elements permits interaction of several widely expressed and IFN-γ-responsive transcriptional activators with cognate binding sites in the *CYBB* proximal promoter. DNA-binding proteins that up-regulate gp91-*phox* expression in myeloid cells include the developmentally-regulated ETS transcription factor PU.1, interferon-regulatory factor 1, and interferon consensus sequence-binding protein, which function cooperatively as a complex termed hematopoiesis-associated factor [Lindsey et al., 2007]. Additional, functionally important binding sites engage transcription factors CP-1, Elf-1, interferon regulatory factor 2, STAT1, and YY-1 [Kumatori et al., 2002]. In addition, a human CpG binding protein binds further upstream, within 1,500 bp of the transcription start site [Voo et al., 2000]. Anrather et al. [2006] identified functional NF-κB binding sites at −1,788 and −1,819 nucleotides upstream from the transcription start site of the murine *Cybb* gene, with homologous—but untested—sites at approximately −3,500 bases in the human *CYBB* promoter.

However, functional studies of the proximal promoter have demonstrated that additional genomic elements are necessary for properly regulated expression of the *CYBB* gene. Lien et al. [1997] showed that fully appropriate regulation in transgenic animals requires a set of distant *cis* elements, represented in four DNase I hypersensitive sites (designated HS-I, II, III, and IV), located respectively at 13, 15, 28, and 29 kb upstream of the *CYBB* transcription start site.

Our previous in vivo and in vitro studies have indicated a functional role for NF-κB in respiratory burst activity and human phagocyte NADPH oxidase gene expression. In vivo, mutations in the *IKBKG* gene, which encodes the NF-κB regulatory protein NEMO, cause anhidrotic ectodermal dysplasia associated with immunodeficiency (EDA-ID; OMIM 300291), a genetic disorder characterized by the aberrant development of skin appendages, including eccrine sweat glands (anhidrosis), as well as severe infections caused by mycobacteria and other microorganisms [Bustamante et al., 2011]. In vitro, EBV-transformed B cells from EDA-ID patients, as well as U937 cells stably transfected with an NF-κB repressor (IκBα-S32A/S36A), showed significantly decreased superoxide release and *CYBB* gene expression [Luengo-Blanco et al., 2008]. Gallin's group has also shown impaired superoxide production in neutrophils from patients with NEMO deficiency [Singh et al., 2009]. However, no functional NF-κB sites have heretofore been shown to regulate human *CYBB* expression.

We now report a putative NF-κB binding site within the HS-II region of the distant 5′ flanking region of the *CYBB* gene, 15 kb upstream from the transcription start site, and provide evidence for the involvement of this distant NF-κB site in the regulation of *CYBB* gene expression in human phagocytes.

MATERIALS AND METHODS

MATERIALS

RPMI 1640 and FBS were purchased from Life Technologies (Gaithersburg, MD); LPS (*Escherichia coli* serotype 026:B6) from Sigma (St. Louis, MO); Lymphoprep from Mycomed (Oslo, Sweden). All reagents (except LPS), serum, buffers and media used for cell preparation and incubation were free of LPS (<0.01 ng/ml by limulus amoebocyte lysate assay; Sigma).

CELL CULTURE AND ISOLATION

HL60 and PLB985 cells [Collins et al., 1977; Tucker et al., 1987] were obtained from R.C. Gallo and T.A. Rado, respectively; U937 and NB4 cells [Larrick et al., 1980; Lanotte et al., 1991] from American Type Culture Collection. Cells were seeded at $1–2 \times 10^5$, and cultured in RPMI 1640 complete medium supplemented with 10% heat inactivated FBS, 2 mM L-glutamine, 100 U/ml penicillin and 100 μg/ml streptomycin, with or without cytokines as indicated. In addition, U937 cells stably transfected with pCMV3 empty vector or pCMV3 containing an IκBα mutant construct (IκB-S32/36) with mutations of two critical serines, S32 and S36, to alanine [Pennington et al., 2001] were kindly provided by Dr. Carlos V. Paya. The cells had been transfected by electroporation of pCMV3 empty vector or pCMV3 containing the IκBα mutant construct. IκB-S32/36, originally obtained as a FLAG-tagged construct in pCMV2, was transferred to pCMV3 plasmid containing an N-terminal (His) 6-encoding sequence and the hygromycin selection cassette from pcDNA3.1 (Invitrogen, Inc.). Transfected clones were selected and maintained in medium containing hygromycin.

Neutrophils and mononuclear cells were isolated from freshly drawn venous blood of healthy male volunteers (30–40 years old) using dextran sedimentation, centrifugation through Ficoll-Hypaque (Lymphoprep), and very brief hypotonic lysis of erythrocytes as previously described [Subrahmanyam et al., 1999]. Morphologically, the neutrophil preparations contained <3% eosinophils and <0.5% monocytes, as assessed by light microscopy. Mixed mononuclear cell preparations from the Ficoll-Hypaque interface, which contained variable proportions of lymphocytes and monocytes, were used without further fractionation in order to avoid activation or maturation of monocytes. Mononuclear cells (1×10^7) or neutrophils (5×10^8) were resuspended in RPMI 1640 for each set of conditions. Neutrophils were incubated with 250 pg/ml LPS for 90 min and mononuclear cells were incubated with LPS 1 ng/ml or TNF-α 1,000 U/ml for 6 h, in the presence and absence of 5 mM salicylate or 20 μM indomethacin, before RNA extraction. Full institutional review board approval for the human studies was obtained at both University of São Paulo and University of Massachusetts Medical School.

ELECTROPHORETIC MOBILITY ASSAYS

HL60 cells (1×10^7) were incubated for 30 min with TNF-α 1,000 units/ml. Nuclear extract preparation was performed essentially as described in Dignam et al. [1983] but with an initial 10-min incubation with 5 μl di-isopropylfluorophosphate. Cells were then washed twice in ice-cold PBS and collected by centrifugation. Cells were resuspended in buffer A (50 mM NaCl, 10 mM HEPES pH 8.0, 500 mM sucrose, 1 mM EDTA, 0.5 mM spermidine, 0.15 mM spermine, 0.2% Triton X-100), and nuclei collected by centrifugation. The nuclear pellet was washed in buffer B (50 mM NaCl, 10 mM HEPES pH 8.0, 25% glycerol, 0.1 mM EDTA, 0.5 mM spermidine, 0.15 mM spermine), before being resuspended in buffer C (350 mM NaCl, 10 mM HEPES pH 8.0, 25% glycerol, 0.1 mM EDTA, 0.5 mM spermidine, 0.15 mM spermine). After a 30-min incubation at 4°C, nuclear debris was removed by centrifugation and the nuclear extract was aliquoted and stored at −80°C. Protein concentration was determined by Bradford assay. Protease inhibitors and β-mercaptoethanol were added to all buffers immediately before use.

Approximately 0.5 ng of γ-^{32}P[ATP] 5′-end labeled oligonucleotide probe (described below) was mixed with 0.012 gel shift units of recombinant human p50 (Promega) or 10 μg of nuclear extract in a total volume of 25 μl containing 25 mM Hepes pH 8.0, 1 mM EDTA, 3.5 mM spermidine, 6 mM $MgCl_2$, 100 mM NaCl, 0.15% NP40, 10% glycerol, 10 mM DTT, 1 mg/ml BSA (Sigma) and 0.5 μg poly(dIdC). After incubation at 20°C for 15 min, anti-p65 or anti-p50 antibodies or non-immune serum (the kind gifts of R.T Hay, University of St. Andrews) were added and after a further 10 min incubation, the protein-bound and unbound probes were separated on 6% native polyacrylamide gels in 0.5 × TBE. Oligonucleotide probes were NFκB cons (NF-κB consensus site, obtained from Promega), NFκB.cybb (*CYBB* putative κB site), and AP-1 consensus site; sequences are listed in the Supplemental Table.

CHROMATIN IMMUNOPRECIPITATION

The ChIP protocol provided by Merck Millipore, Inc. (Billerica, MA) was followed, with the following modifications, using 5×10^7 HL-60 cells for each cross-linking reaction. Glycine (1 M stock) was added to a final concentration of 125 mM to quench crosslinking after the formaldehyde incubation, and then centrifugation was performed at 200*g* for 4 min at 4°C. Antibody precipitations were performed with a combination of Upstate (Merck Millipore) anti-p50 (5 μg) and anti-p65 (2 μg) antibodies and a no-antibody control. After reversal of cross-linking and proteinase K treatment, samples were dissolved in 25 μl distilled water for PCR analysis.

Immunoprecipitated DNA was tested for the presence of the putative κB site, as well as for the NF-κB-binding region of the I-κB promoter and exon 9 of the *CYBB* gene as positive and negative controls, respectively. Nested PCR was performed with a first reaction using 2 μl of the immunoprecipitate as template in 20 cycles of amplification in a 50 μl reaction mix; followed by PCR with internal primers using 5 μl of the first reaction product for 30 cycles of amplification in a 25 μl reaction mix. Products of the second reaction were analyzed by electrophoresis of 5 μl samples on 2% agarose gels and stained with SYBR green. Primer sequences are listed in the Supplemental Table.

CHROMOSOME CONFORMATION CAPTURE

3C assays [Dekker et al., 2002] were performed as previously described [Naumova et al., 2012] with the following modifications. 3C restriction fragments were defined by BglII enzyme digestion. The anchor primer queried the region of the NF-κB site, using sequence close to the nearest BglII site at X chromosome position 37511756 (hg18; See the Supplemental Table for all BglII sites and primers). Approximately 1×10^8 NB4 cells were fixed with 1% formaldehyde in RPMI with 10% FBS for 10 min at room temperature. Formaldehyde was quenched by the addition of 0.125 M glycine. Nuclei were released by Dounce homogenization in ice-cold lysis buffer (10 mM Tris–HCl pH 8.0, 10 mM NaCl, 0.2% NP-40) containing Protease Inhibitor Cocktail (Sigma). Nuclei were collected and subjected to overnight digestion with 400 U of BglII (New England BioLabs, Ipswich, MA). The enzyme reaction was halted by incubation at 65°C for 30 min in the presence of 10% sodium dodecyl sulphate. Samples were aliquoted into 20 separate tubes and were diluted 40-fold in ligation buffer and subjected to proximity-mediated ligation with 10 U of T4 DNA Ligase (Invitrogen, Life Technologies, Grand Island, NY) per reaction for 4 h at 16°C. Cross linking of nuclear material was reversed by overnight incubation with 50 μl Proteinase K (10 mg/ml, Roche) at 65°C. Ligated chromatin was extracted by phenol-chloroform extraction followed by ethanol precipitation. Optimal amounts of experimental library and bacterial artificial chromosome (BAC) control templates for PCR reactions were determined by titration experiments to find template concentrations from the range that produced linear slopes for PCR signal. A set of 28- to 34-mer 3C primers spanning the *CYBB* gene locus were designed by Primer3 software to annealing temperatures of 63 ± 1°C; sequences are listed in the Supplemental Table. PCR conditions were 95°C for 5 min followed by 35 cycles of 95°C for 30 s, 63°C for 30 s and 72°C for 30 s, followed by 95°C for 30 s, 63°C for 30 s, and 72°C for 8 min. All 3C PCR products were analyzed on 2% agarose gels stained with ethidium bromide; signal quantitation was performed with a ChemiDoc imaging system (Bio-Rad).

Interaction frequencies were determined by assessing fold change of 3C PCR amplification product of sample chromatin compared to randomly ligated BglII-digested BAC clone RP11-299O2 (obtained from Children's Hospital Oakland Research Institute) that spans the *CYBB* locus. Interaction frequency was calculated by dividing the amount of PCR product from the 3C template by the amount of PCR product from the BAC control template, thereby normalizing for differences in primer efficiencies. All of the 3C primer pairs yielded similar amounts of product with both the 3C and the BAC templates. Ligation efficiencies of all 3C samples were normalized to each other by comparison to the average of the ligation frequencies of the most distant CYBB BglII site (X chromosome position 37557276) for each set of technical replicates from each 3C library. Primers that gave very low PCR yields were discarded. 3C data represent the averaged ligation frequencies of two independent cultures and library preparations, with three technical replicates for each.

NF-κB INHIBITION BY IκB-S$^{32/36}$

U937 cells containing the IκBα mutant construct (IκB-S$^{32/36}$) with mutations of critical serines S^{32} and S^{36} to alanine [Asin et al., 1999; Pennington et al., 2001] were cultured as described above and

differentiated by incubation for 72 h in 1 mM dibutyryl cAMP [Sheth et al., 1988]. Persistent, high-level repression NF-κB function by IκB-$S^{32/36}$ was confirmed by testing NF-κB-driven expression of a transiently expressed luciferase reporter. PLB985 cells containing either the empty vector or IκB-$S^{32/36}$ were electroporated with 10 μg each of plasmid pLuc-MCS (Stratagene, Inc.) containing the firefly luciferase gene driven by five tandem NF-κB consensus recognition sites and plasmid pHRL-TK (Promega, Inc.) containing the Renilla luciferase gene driven by the HSV thymidine kinase promoter. Relative expression of the firefly and Renilla luciferase proteins was assessed by the Dual-Glo™ Luciferase Assay System (Promega).

RNA EXTRACTION AND ANALYSIS

Total cellular RNA was isolated from neutrophils using guanidine HCl as previously described [Subrahmanyam et al., 1999]. RNA was analyzed by standard northern blot procedures [Gatti et al., 1984], using radiolabeled cDNA complementary to the *CYBB* gene and a normalization probe complementary to 18s rRNA, as previously described [Newburger et al., 1991]. Quantitative measurements of hybridization were performed by phosphorimager analysis. Alternatively, transcript levels were assessed by PCR assays, as described below.

RT-PCR

Total RNA was isolated from U937 cells (5×10^6 cells/ml) by TRIzol® Reagent (Life Technologies), according to manufacturer's instructions. Reverse transcription was performed on 3 μg of RNA with SuperScript II RT (Life Technologies) from random hexamers. The cDNA was amplified by 30 cycles of PCR with oligonucleotides specific for gp91-*phox* (Gene Bank NM 00397) or β-actin (Gene Bank NM 001101) as previously described [Luengo-Blanco et al., 2008]. PCR products were analyzed by agarose electrophoresis and ethidium bromide staining, and quantitated by digital photograph and computer analysis with Molecular Analyst software (Bio-Rad). Levels of gp91-*phox* transcripts were adjusted for cDNA normalized to β-actin signals from the same cDNA preparations.

PROMOTER/LUCIFERASE REPORTER

U937 cells (1×10^6/ml), untreated or previously incubated with IFN-γ 100 units/ml for 24 h were transfected with both a CMV promoter/Renilla luciferase (pRL-CMV) transfection control and a reporter construct containing the firefly luciferase gene on a backbone derived from the pCMV/Bsd/Luc plasmid (Promega). In these constructs, the CMV promoter was replaced by the 1,500 bp proximal promoter sequence from *CYBB*, formed by PCR amplification from −1,500 to +3 relative to the transcription start site, plus the *CYBB* NF-κB site, native (ggaaagcccc) or scrambled (cagacggagc), inserted as oligonucleotides immediately 3′ to the 1,500 bp promoter region (pBsd/NFκB/−1,500/Luc and pBsd/scramble/−1,500/Luc, respectively). In addition, cells were transfected with either pCMV4-3 HA/IkB-alpha(SS32,36AA) (Addgene plasmid #24143; functionally equivalent to the IκB-$S^{32/36}$ construct described above) or the empty vector pCMV4-3 HA. Following transfection using the Amaxa Cell Line Nucleofector Kit C for U937 (Lonza), cells were incubated for 48 h with or without IFN-γ. Luciferase expression was then measured with the Dual-Luciferase Reporter Assay System (Promega) following the manufacturer's instructions. All samples were read in a GloMax® 96 Microplate Luminometer with Dual Injectors. Ratios of firefly to Renilla luciferase luminescence in six independent experiments were calculated as means and SEMs and analyzed using the one-tailed Mann–Whitney test; significance was determined at $P < 0.05$.

RESULTS

The *CYBB* 1,500 bp proximal promoter region has been well characterized (22,46–50) and does not contain any known NF-κB recognition sites. However, our analysis of DNA sequence in the areas of the upstream DNase-I hypersensitive sites (Lien et al., 1997) using tools on the Transfac web site (http://www.gene-regulation.com/pub/databases.html#transfac) identified one putative NF-κB binding site in DNase-I hypersensitive site II (HS-II), 15 kb upstream of the *CYBB* transcriptional start site (Fig. 1). The NF-κB binding sequence 5′-GGGGCTTTCC-3′ is on the antisense DNA strand and is identical to a heterodimeric NF-κB binding site found in the TNF-α promoter, 510 bp upstream from that transcription start site [Chen and Ghosh, 1999].

Gel shift experiments (Fig. 2, panel A) demonstrated that recombinant human p50 (rh-p50) specifically binds to the putative NF-κB site in HS-II. Radiolabeled 22 bp oligonucleotide representing the *CYBB* κB site forms a shifted complex with rh-p50 (lane 2). This complex is efficiently competed away by a 100-fold excess of unlabeled NF-κB oligonucleotide corresponding to the site identified in *CYBB* (lane 4) and also by NF-κB consensus oligonucleotide (lane 3). The latter sequence differs by only one nucleotide from the κB site in *CYBB* (see sequences in Materials and Methods). In contrast, oligonucleotide corresponding to an unrelated transcription factor (AP-1) binding site fails to compete for rh-p50 binding (lane 5).

The *CYBB* distant upstream κB sequence is also specifically bound by the forms of NF-κB that are induced in HL-60 cells as a result of TNF-α stimulation. Gel shift assays illustrated in Figure 2, panel B, revealed two probe-specific bands (A and B in the figure). Band A appears to be constitutively present and its level is unaffected by TNF-α stimulation, as indicated by its presence in both lanes 2 and 3. Binding of this protein complex to the probe DNA sequence is highly specific, demonstrated by competition from excess sequence-

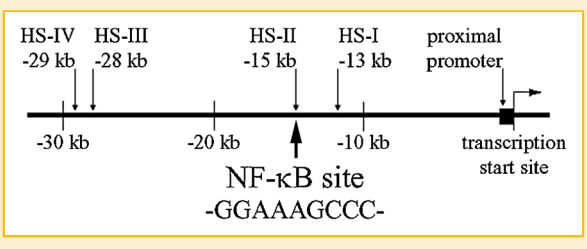

Fig. 1. Location of the putative NF-κB binding site upstream from the *CYBB* gene. The schematic diagram indicates the positions of DNase-I hypersensitive sites (HS) I, II, III, and IV;(25) the NF-κB site within HS-II; and the transcription start site.

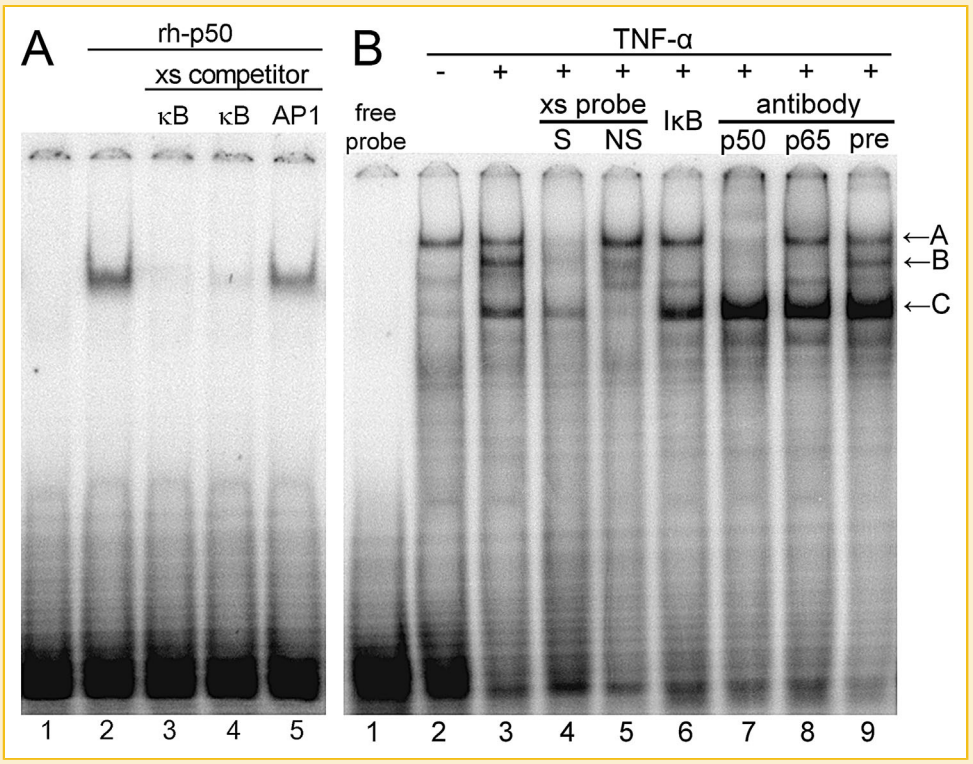

Fig. 2. Gel shift analysis of the putative *CYBB* NF-κB site. Panel A: Binding of recombinant human p50. ^{32}P-5′end-labeled NFκB.cybb oligonucleotide (0.5 ng, 0.035 pmol) was incubated with rh-p50 (0.012 gel shift units) and analyzed by electrophoresis on a native polyacrylamide gel. Lane 1: free probe. Lanes 2–5: probe plus rh-p50. Lanes 3 and 4 contain a 100-fold excess of unlabeled specific competitors: NF-κB consensus sequence (NFκB.cons) and *CYBB* NF-κB site (NFκB.cybb), respectively. Lane 5 contains a 100-fold excess of non-specific competitor DNA containing an AP-1 binding site. Panel B: Binding of HL-60 nuclear extract. End labeled NFκB.cybb probe was incubated with nuclear extract from HL-60 cells with or without TNF-α treatment, as indicated in the top margin, and then analyzed by electrophoresis on a native polyacrylamide gel. Incubations also included, as indicated above the image. Lanes 4 and 5: excess unlabeled oligonucleotide representing specific ("S": NFκB.cons) or non-specific ("NS": AP-1) competitors. Lane 5: recombinant human I-κBα. Lanes 7–9: antibody to human p50 or p65, or preimmune IgG, as indicated. Labels in the right margin indicate bands A, B, and C as discussed in the text. The images are each representative of three independent experiments.

specific unlabeled probe (lane 4) but not by non-specific unlabeled probe (lane 5). Band A appears to contain p50, shown by its absence after addition of anti-p50 antibody (lane 7), but does not contain p65, as it is unaffected by the addition of anti-p65 antibody (lane 8). Also, its ability to bind DNA appears unaffected by the presence of IκB-α, which is less inhibitory to complex formation by p50 homodimers than to p50/p65 heterodimers. Neither band A nor B is affected by the incubation with pre-immune serum (lane 9).

However, band B in Figure 2, panel B, is induced by TNF-α stimulation (lanes 2 and 3). This complex also binds the *CYBB* NF-κB DNA probe specifically (lanes 4 and 5), and appears to include both p50 (lane 7) and p65 (lane 8). Binding of band B to the probe is inhibited by incubation with IκB-α (lane 6). These characteristics indicate that band B represents a p50–p65 heterodimer/DNA complex. Nuclear p50–p65 heterodimers have been reported previously to be induced in neutrophils upon LPS or TNF-α stimulation [McDonald et al., 1997]. The identity of band C is unknown, though it does not seem to represent a member of the Rel homology family. Although it is induced by TNF-α (lanes 2 and 3), its ability to bind the probe is non-specific (lanes 4 and 5) and it is unaffected by the presence of IκB-α or by the anti-p50 and -p65 antibodies (lanes 6, 7 and 8).

In order to test whether binding of NF-κB protein to the putative κB site in HS-II occurs in intact myeloid cells, we performed chromatin immunoprecipitation (ChIP) in HL-60 cells. As shown in Figure 3, DNA from the *CYBB* upstream κB site could be amplified from protein–DNA complexes immunoprecipitated with a mixture of antibodies to p50 and p65 (top panel, lane 2), as could the well-characterized NF-κB binding site in the promoter of the IκBα gene (bottom panel, lane 2). There was no detectable immunoprecipitated DNA from *CYBB* exon 9 (middle panel, lane 2), which served as a negative control for non-specific immunoprecipitation of *CYBB* DNA. No signal was detected in the absence of specific antibody or of DNA template (lanes 3–5).

To test for physical association of the *CYBB* NF-κB binding site with the promoter and gene 15 kb downstream, we performed 3C assays [Dekker et al., 2002] in NB4 myeloid leukemia cells to measure interaction frequencies between the site and multiple points in the *CYBB* genomic region. As shown in Figure 4, the anchor oligonucleotide probe, located near the κB site, showed the expected high interaction frequency with genomic DNA at neighboring BglII sites. The interaction frequency then fell, as expected, in both directions, but then rose again, showing strong interactions with the *CYBB* proximal promoter region and 5′ region of the gene. This

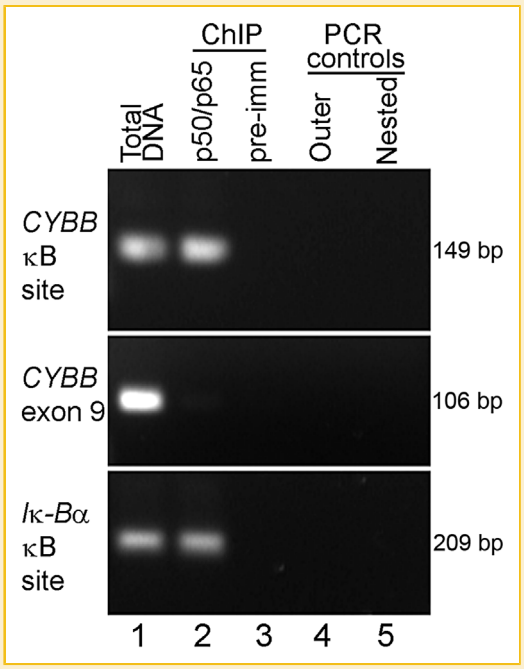

Fig. 3. ChIP-PCR analysis of the distant upstream NF-κB site. Protein–DNA complexes immunoprecipitated by anti-p50 and anti-p65 from HL-60 cells were analyzed by PCR amplification of the *CYBB* NF-κB binding site, *CYBB* exon 9 (negative control), and the IκBα NF-κB binding site (positive control) with nested primers. PCR templates were derived, as indicated in the top margin, from total cellular DNA, ChIP with anti-NF-κB antibodies or control immunoglobulin. Template-free PCR controls are shown for the outer and nested set of primers. The image is representative of three independent experiments.

pattern is characteristic for enhancer elements that affect expression of distant genes [Miele and Dekker, 2008; Naumova et al., 2012].

To test the functional role of NF-κB in *CYBB* expression, we examined the effect of salicylate on the steady state level of *CYBB* transcripts in primary human phagocytes. Salicylate and indomethacin are non-steroidal anti-inflammatory drugs that exert their effects at least in part by inhibition of cyclooxygenase [Vane, 1994]. Salicylate, however, also inhibits the NF-κB pathway by specifically supressing ATP binding activity of inhibitor of NF-κB kinase, subunit beta (IKKβ) [Yin et al., 1998]. Although indomethacin showed partial inhibition of NF-κB in a single study [Shen et al., 2007], their doses were 5- to 50-fold higher than those used here and in our previous studies, which showed no effect of the drug on NADPH oxidase activity or gene expression [Condino-Neto et al., 1998]. As shown in Figure 5, *CYBB* gene expression in human peripheral blood neutrophils stimulated with LPS, assayed by northern blot (left panel, upper image) and quantitative phosphorimager analysis (right panel, upper image), showed a small but consistent increase in transcript levels, as previously reported [Newburger et al., 1991]. This stimulation was abrogated by salicylate, but not by indomethacin, indicating that the effect is not due to inhibition of the cyclooxygenase pathway. However, this effect of salicylate was not observed in peripheral blood mononuclear cells (left and right panels, lower images), which may indicate the presence of greater redundancy in the signal transduction and transcription pathways in these cells.

For more specific inhibition of NF-κB function, we used stably transfected human macrophage-like cell line U937 expressing a construct expressing inhibitor of κB (I-κB) mutated at serines S32 and S36 to ablate its phosphorylation sites, making it a dominant

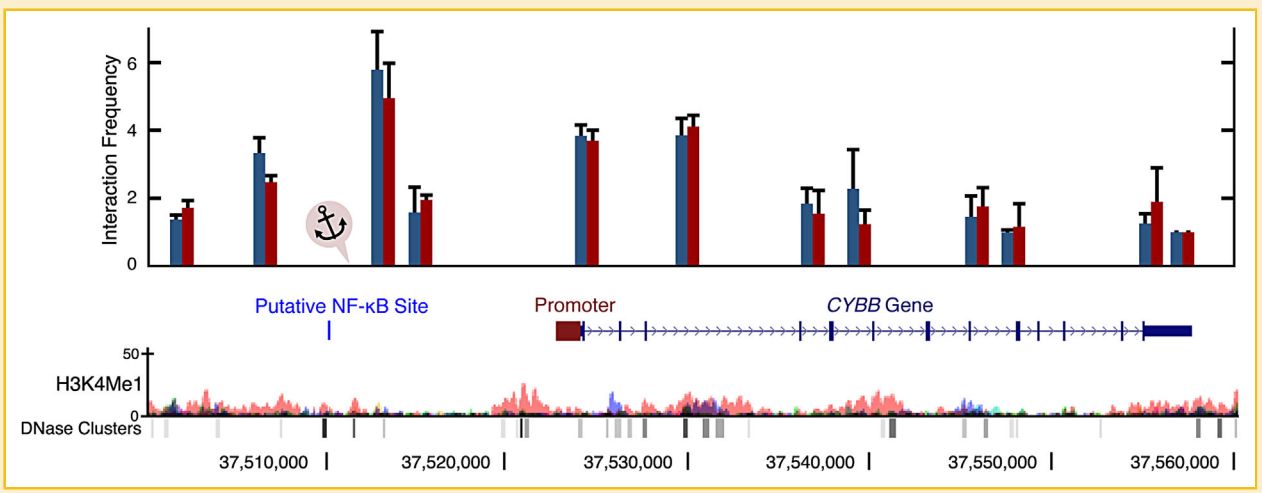

Fig. 4. Chromosome conformation capture (3C) analysis of interactions between the NF-κB site and the *CYBB* genomic region in NB4 cells. Bars and error brackets indicate mean and SD for interaction frequencies of the anchor primer (so indicated) with primers at the indicated genomic positions, with the most distal primer interaction defined as frequency = 1 (bars and error brackets represent mean ± SD of triplicate PCR amplifications for two biological replicates, indicated by blue and red bars). The positions of the putative NF-κB site and *CYBB* gene elements mapped on a UCSC genome browser image (http://genome.ucsc.edu/cgi-bin/hgTracks?db=hg18&position=chrX%3A37500000–37560000) showing (bottom to top) X chromosome genomic scale, DNase I hypersensitive sites (University of Washington DNaseI Hypersensitivity by Digital DNaseI data, including myeloid cell lines K562 and NB4, and GM12878, a lymphoblastoid B cell line that weakly expresses *CYBB*), and enhancer- and promoter-associated histone mark H3K4Me1 (mono-methylation of lysine 4 of the H3 histone protein; ENCODE data from eight cell lines, including GM12878 in salmon color).

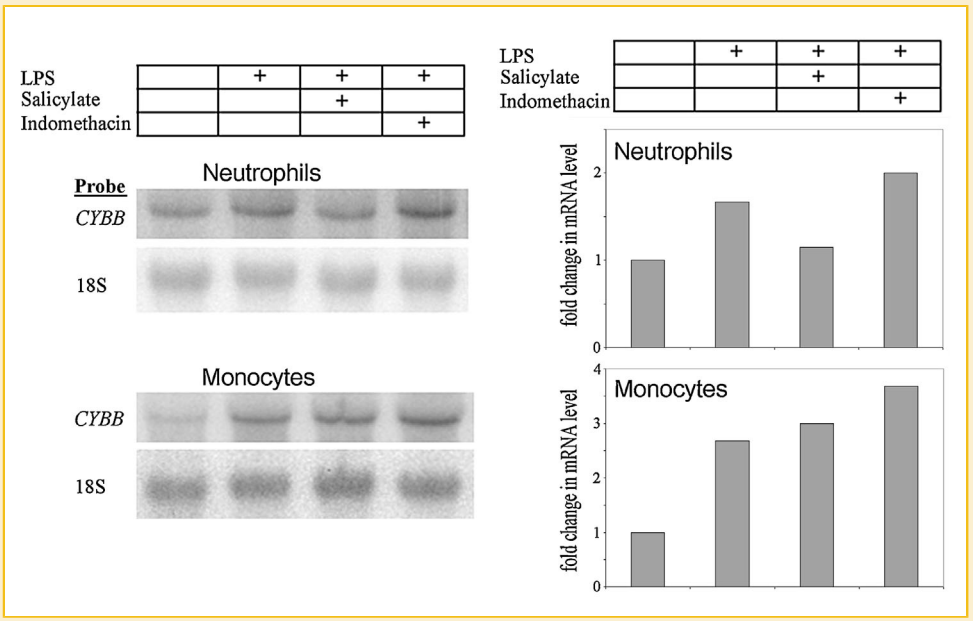

Fig. 5. Effect of NF-κB inhibitors on *CYBB* expression in response to LPS. Left Panel: Northern blot analysis of RNA from human peripheral blood neutrophils (upper lanes) and monocytes (lower lanes), treated with LPS, salicylate, or indomethacin as indicated in the overlying grid. RNA was probed with radiolabeled cDNA complementary to the *CYBB* gene or a normalization probe complementary to 18s RNA, as indicated in the left margin. The images are representative of three independent experiments. Right Panel: Quantification of data from a representative northern blot experiment. The bars indicate the fold change of *CYBB* transcript levels (normalized to levels of 18s rRNA) in neutrophils (upper graph) and monocytes (lower graph) treated with LPS, salicylate, or indomethacin as indicated in the overlying grid.

negative "super-repressor" [Pennington et al., 2001]. Figure 6 shows *CYBB* expression in these cells, with or without differentiation along the monocytic pathway induced by incubation with dibutyryl cAMP [Sheth et al., 1988]. Native U937 cells show expression of *CYBB* (lane 1) that is up-regulated by cAMP (lane 2). A similar pattern is evident in U937 cells transfected with empty vector (lanes 3 and 4). However, cells transfected with mutant I-κB "super-repressor" showed markedly diminished *CYBB* expression (lanes 5 and 6), although some cAMP induction was still present.

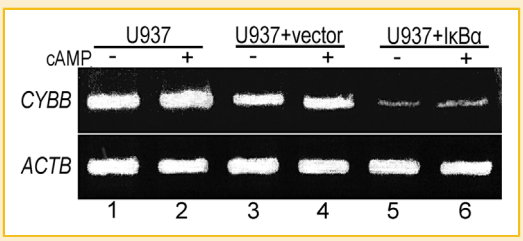

Fig. 6. RT-PCR analysis of *CYBB* expression in U937 cells transfected with I-κB "super-repressor." Total RNA from U937 cells was analyzed by RT-PCR as described in Materials and Methods. The panels show gel electrophoresis bands of amplicons from the *CYBB* and *ACTB* (β-actin) genes, as indicated. Lanes 1 and 2: native U937 cells. Lanes 3 and 4: U937 cells transfected with empty vector. Lanes 5 and 6: U937 cells transfected with IκBα "super-repressor" (serine to alanine mutations at serines 32 and 36). Lanes 2, 4, and 6: cells induced to monocytic differentiation with dibutyryl cAMP.

We also directly measured the enhancer function of the NF-κB site on the *CYBB* promoter by means of a luciferase reporter assay. We analyzed the relative expression in the U937 cell line of two luciferase reporter plasmids: pCMV-Bsd-Luc-NFκB-1,500 carrying the putative *CYBB* upstream NFκB sequence and *CYBB* 1,500 bp proximal promoter driving the luciferase gene, and pCMV-Bsd-Luc-scramble-1,500 containing a scrambled sequence of the NF-κB site; these constructs were co-transfected with either the I-κB "super-repressor" or empty vector. The cells were also incubated with or without IFN-γ, a cytokine that strongly up-regulates *CYBB* in vitro and in vivo [Newburger et al., 1988] and is known in other systems to activate NF-κB, most likely by indirect mechanisms [Lin et al., 2012]. As shown in Figure 7, expression of luciferase was slightly but significantly ($P < 0.05$; one-tailed Mann–Whitney test) higher in cells transfected with the construct containing the native NF-κB sequence (lanes 2 and 6) than the scrambled sequence (lanes 1 and 5), and the effect was abrogated by the I-κB repressor (lanes 3–4, 7–8). Results were similar in untreated cells (lanes 1–4) or those incubated with IFN-γ for 24 h prior to transfection (lanes 5–8). Further treatment with IFN-γ for 48 h significantly augmented luciferase expression (lane 2 vs.10).

DISCUSSION

We have identified, by sequence analysis, a novel NF-κB binding site within HS-II, a DNase-I hypersensitive site situated 15 kb upstream of the *CYBB* transcriptional start site. The putative NF-κB binding

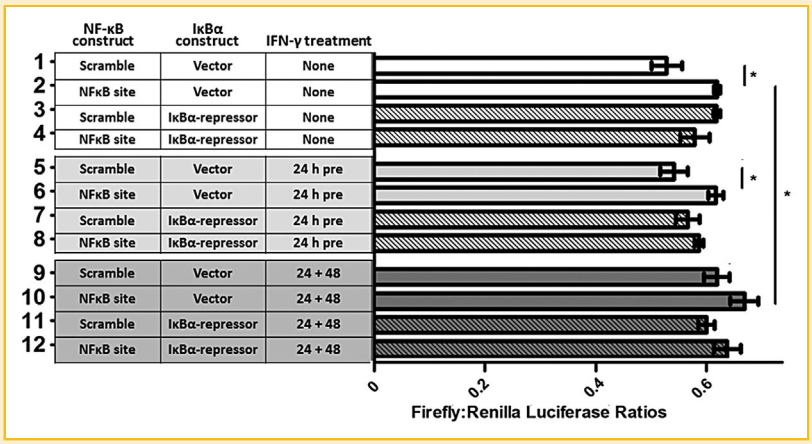

Fig. 7. Expression of luciferase reporters driven by the *CYBB* proximal promoter with the native or scrambled NF-κB binding sequence. U937 cells transfected, as indicated, with either pCMV-Bsd-Luc-NFκB-1,500 carrying the putative *CYBB* upstream NF-κB sequence and *CYBB* 15,00 bp proximal promoter driving the luciferase gene, or pCMV-Bsd-Luc-scramble-1,500, containing a scrambled sequence of the NF-κB site. In addition, cells were cotransfected, as indicated, with either pCMV4-3HA-kBa expressing the IκBα "super-repressor" or with the empty vector pCMV4-3HA. These combinations of transfectants were incubated, as indicated, with no cytokine or with IFN-γ for 24 h before transfection or with IFN-γ for 24 h and a further 48 h after transfection. The bars and error brackets represent means and SEMs of six independent experiments; asterisks indicate significance at $P < 0.05$ (one-tailed Mann–Whitney test) for comparison of data from the groups plotted at each end of the vertical line.

sequence, GGGGCTTTCC, corresponds to the consensus binding sequence GGGRNNYYCC (R = purine, Y = pyrimidine, N = any base) [Rothwarf and Karin, 1999], and is identical to a heterodimeric NF-κB binding site found in the TNF-α promoter [Chen and Ghosh, 1999]. The five mammalian NF-κB family members (p50, p52, RelA/p65, RelB, and c-rel) function either as homo- or heterodimers, but differ in their ability to activate transcription and exhibit varying binding affinities for κB sites [Bhatt and Ghosh, 2014].

In our current study, electrophoretic mobility assays showed that the sequence element binds recombinant NF-κB protein p50. Gel shift experiments using nuclear extract from the HL-60 myeloid cell line demonstrated a shifted band that was disrupted anti-p50 antibody, thus confirming p50 binding, and a second band whose formation was inhibited by both IKB-α and anti-p50 antibody, indicating the participation of p50/p65 heterodimers. ChIP experiments verified these in vitro assays by demonstrating NF-κB binding to the *CYBB* HS-II κB site in intact HL-60 cells.

Binding sites for NF-κB proteins are widely distributed in the human genome. In a "ChIP–chip" study of p65 binding, using chromatin immunoprecipitation from HeLa cells analyzed on a genomic tiling microarray of human chromosome 22 DNA, binding sites were identified in both coding and noncoding regions, including introns [Martone et al., 2003]. Not only was p65 binding not restricted to promoter regions, but it was also associated with genes whose expression was not altered by incubation with TNF-α, suggesting that NF-κB binding alone is not sufficient for gene activation. Nine percent of the p65 binding sites on chromosome 22 are located 5–10 kb upstream from the transcription start sites of annotated genes [Martone et al., 2003]. Functional analysis of a κB enhancer element 2.3 kb upstream from the monocyte chemoattractant protein 1 gene (*MCP1*) suggest that the distance of the enhancer from the proximal promoter permits maintenance of two independent chromatin states at the enhancer and promoter regions, so that NF-κB binding at the former affords priming or readiness, but actual transcription depends on additional signals at the proximal promoter [Teferedegne et al., 2006].

Our 3C data indicate a long-distance physical interaction between the NF-κB binding site and the *CYBB* proximal promoter and gene sequences, most probably by chromatin looping typical of transcriptional enhancer activity (Miele and Dekker, 2008). Functional studies of NF-κB in *CYBB* expression also support the hypothesis that the upstream site acts as an enhancer element that modifies gene expression, rather than as an essential promoter element with absolute regulatory function. In experiments testing the effects of NF-κB inhibitors on *CYBB* transcript levels, treatment with salicylate led to a partial reduction of *CYBB* expression in peripheral blood neutrophils and differentiated U937 cells, although not in peripheral blood mononuclear cells. In addition, U937 cells transfected with mutant IκBα-S32A/S36A "super-repressor" showed partial, but significant, decreases in *CYBB* expression, and a luciferase reporter assay showed enhanced function of the *CYBB* promoter by the upstream NF-κB sequence.

These results provide a basis for our previous finding that NF-κB is necessary for full *CYBB* gene expression and activation of the phagocyte NADPH oxidase [Luengo-Blanco et al., 2008]. In that study, U937 cells stably transfected with the IκBα "super-repressor" showed significantly lower superoxide release and *CYBB* (as well as *NCF1*) gene expression compared to controls. In addition, EBV-transformed B cells from patients with EDA-ID (an inherited disorder of NF-κB function) [Bustamante et al., 2011] demonstrated very low levels of superoxide release and *CYBB* gene expression, equivalent to cells from X-linked CGD patients. These results complement the functional studies of NF-κB activation in murine phagocytes [Anrather et al., 2006] and demonstrate that a defect in NF-κB activation results in loss of phagocyte oxidase activity in a human immunodeficiency disorder. The greater loss of *CYBB* expression and

oxidase activity in genetic disorders suggests, not surprisingly, that NF-κB plays a much broader role in phagocyte development and function, beyond its binding to this single enhancer site.

The identification and functional characterization of this upstream NF-κB binding site indicate an enhancer function for the element and represent the first specific protein–DNA interaction identified within the set of four distant DNase I hypersensitive sites located upstream from the *CYBB* gene [Lien et al., 1997]. The present studies also provide a molecular basis for the physiological and clinical findings that NF-κB function is necessary for the activation of the phagocyte NADPH oxidase and help explain previous findings, by our group and others, of deficient oxidase activity in EDA-ID, [Luengo-Blanco et al., 2008; Singh et al., 2009] a primary immunodeficiency disease of the NF-κB pathway [Bustamante et al., 2011].

ACKNOWLEDGMENTS

We thank Dr. Stuart Orkin for providing DNase I hypersensitive site sequence data; Dr. Carlos V. Paya for one of the IκBα mutant constructs; Professor R. T. Hay and Ye Zhan, MS, for reagents and advice; Jussara Rehder for technical assistance; and Melody Lu and Daniel Newburger for creating the 3C figure.

REFERENCES

Anrather J, Racchumi G, Iadecola. C. 2006. NF-kappaB regulates phagocytic NADPH oxidase by inducing the expression of gp91phox. J Biol Chem 281:5657–5667.

Asin S, Taylor JA, Trushin S, Bren G, Paya CV. 1999. Ikappakappa mediates NF-kappaB activation in human immunodeficiency virus-infected cells. J Virol 73:3893–3903.

Bei L, Lu Y, Bellis SL, Zhou W, Horvath E, Eklund EA. 2007. Identification of a HoxA10 activation domain necessary for transcription of the gene encoding beta3 integrin during myeloid differentiation. J Biol Chem 282:page-First>16846–16859.

Bhatt D, Ghosh S. 2014. Regulation of the NF-kappaB-mediated transcription of inflammatory genes. Front Immunol 5:71.

Bustamante J, Picard C, Boisson-Dupuis S, Abel L, Casanova JL. 2011. Genetic lessons learned from X-linked mendelian susceptibility to mycobacterial diseases. Ann NY Acad Sci 1246:92–101.

Chen FF, Ghosh G. 1999. Regulation of DNA binding by Rel/NF-kappaB transcription factors: Structural views. Oncogene 18:6845–6852.

Collins SJ, Gallo RC, Gallagher RE. 1977. Continuous growth and differentiation of human myeloid leukaemic cells in suspension culture. Nature 270:347–349.

Condino-Neto A, Whitney C, Newburger PE. 1998. Dexamethasone but not indomethacin inhibits human phagocyte nicotinamide adenine dinucleotide phosphate oxidase activity by down-regulating expression of genes encoding oxidase components. J Immunol 161:4960–4967.

de Oliveira-Junior EB, Bustamante J, Newburger PE, Condino-Neto A. 2011. The human NADPH oxidase: Primary and secondary defects impairing the respiratory burst function and the microbicidal ability of phagocytes. Scand J Immunol 73:420–427.

Dekker J, Rippe K, Dekker M, Kleckner N. 2002. Capturing chromosome conformation. Science 295:1306–1311.

Dignam JD, Lebovitz RM, Roeder RG. 1983. Accurate transcription initiation by RNA polymerase II in a soluble extract from isolated mammalian nuclei. Nucleic Acids Res 11:1475–1489.

Eklund EA, Luo W, Skalnik DG. 1996. Characterization of three promoter elements and cognate DNA binding protein(s) necessary for IFN-gamma induction of gp91-phox transcription. J Immunol 157:2418–2429.

Gatti RA, Concannon P, Salser W. 1984. Multiple use of Southern blots. Biotechniques 2:148–155.

Gauss KA, Nelson-Overton LK, Siemsen DW, Gao Y, DeLeo FR, Quinn MT. 2007. Role of NF-kappaB in transcriptional regulation of the phagocyte NADPH oxidase by tumor necrosis factor-alpha. J Leukoc Biol 82:729–741.

Hawkins SM, Kohwi-Shigematsu T, Skalnik DG. 2001. The matrix attachment region-binding protein SATB1 interacts with multiple elements within the gp91phox promoter and is down-regulated during myeloid differentiation. J Biol Chem 276:44472–44480.

Karimi G, Houee Levin C, Dagher MC, Baciou L, Bizouarn T. 2014. Assembly of phagocyte NADPH oxidase: A concerted binding process?. Biochim Biophys Acta 1840:3277–3283.

Kumatori A, Yang D, Suzuki S, Nakamura M. 2002. Cooperation of STAT-1 and IRF-1 in interferon-gamma-induced transcription of the gp91(phox) gene. J Biol Chem 277:9103–9111.

Lanotte M, Martin-Thouvenin V, Najman S, Balerini P, Valensi F, Berger R. 1991. NB4, a maturation inducible cell line with t(15;17) marker isolated from a human acute promyelocytic leukemia (M3). Blood 77:1080–1086.

Larrick JW, Fischer DG, Anderson SJ, Koren HS. 1980. Characterization of a human macrophage-like cell line stimulated in vitro: A model of macrophage functions. J Immunol 125:6–12.

Lien LL, Lee Y, Orkin. SH. 1997. Regulation of the myeloid-cell-expressed human gp91-phox gene as studied by transfer of yeast artificial chromosome clones into embryonic stem cells: Suppression of a variegated cellular pattern of expression requires a full complement of distant cis elements. Mol Cell Biol 17:2279–2290.

Lin Y, Jamison S, Lin W. 2012. Interferon-gamma activates nuclear factor-kappa B in oligodendrocytes through a process mediated by the unfolded protein response. PLoS ONE 7:e36408.

Lindsey S, Huang W, Wang H, Horvath E, Zhu C, Eklund EA. 2007. Activation of SHP2 protein-tyrosine phosphatase increases HoxA10-induced repression of the genes encoding gp91(PHOX) and p67(PHOX). J Biol Chem 282: 2237–2249.

Luengo-Blanco M, Prando C, Bustamante J, Aragao-Filho WC, Pereira PV, Rehder J, Padden C, Casanova JL, Newburger PE, Condino-Neto A. 2008. Essential role of nuclear factor-kappaB for NADPH oxidase activity in normal and anhidrotic ectodermal dysplasia leukocytes. Blood 112:1453–1460.

Martone R, Euskirchen G, Bertone P, Hartman S, Royce TE, Luscombe NM, Rinn JL, Nelson FK, Miller P, Gerstein M, Weissman S, Snyder M. 2003. Distribution of NF-kappaB-binding sites across human chromosome 22. Proc Natl Acad Sci USA 100:12247–12252.

McDonald PP, Bald A, Cassatella MA. 1997. Activation of the NF-kappaB pathway by inflammatory stimuli in human neutrophils. Blood 89: 3421–3433.

Miele A, Dekker J. 2008. Long-range chromosomal interactions and gene regulation. Mol Biosyst 4:1046–1057.

Naumova N, Smith EM, Zhan Y, Dekker J. 2012. Analysis of long-range chromatin interactions using chromosome conformation capture. Methods 58:192–203.

Nauseef WM, Borregaard N. 2014. Neutrophils at work. Nat Immunol 15: 602–611.

Newburger PE, Dai Q, Whitney C. 1991. In vitro regulation of human phagocyte cytochrome b heavy and light chain gene expression by bacterial lipopolysaccharide and recombinant human cytokines. J Biol Chem 266:16171–16177.

Newburger PE, Ezekowitz RA, Whitney C, Wright J, Orkin SH. 1988. Induction of phagocyte cytochrome b heavy chain gene expression by interferon gamma. Proc Natl Acad Sci USA 85:5215–5219.

Pennington KN, Taylor JA, Bren GD, Paya CV. 2001. IkappaB kinase-dependent chronic activation of NF-kappaB is necessary for p21(WAF1/Cip1) inhibition of differentiation-induced apoptosis of monocytes. Mol Cell Biol 21:1930–1941.

Roos D, de Boer M. 2014. Molecular diagnosis of chronic granulomatous disease. Clin Exp Immunol 175:139–149.

Rothwarf DN, Karin M. 1999. The NF-kappa B activation pathway: A paradigm in information transfer from membrane to nucleus. Sci STKE 1999:RE1.

Shen Y, Yang T, Wang J, Xu Q, Li R, Pan W, Li G, Wang Z, Tan J, Wu J, Wu F, Wang L, Liu Y. 2007. Indomethacin enhances the cytotoxicity of recombinant human lymphotoxin alpha on tumor cells by suppressing NFkappaB signaling. Cancer Biol Ther 6:1428–1433.

Sheth B, Dransfield I, Partridge LJ, Barker MD, Burton DR. 1988. Dibutyryl cyclic AMP stimulation of a monocyte-like cell line, U937: A model for monocyte chemotaxis and Fc receptor-related functions. Immunology 63:483–490.

Singh A, Zarember KA, Kuhns DB, Gallin JI. 2009. Impaired priming and activation of the neutrophil NADPH oxidase in patients with IRAK4 or NEMO deficiency. J Immunol 182:6410–6417.

Subrahmanyam YV, Baskaran N, Newburger PE, Weissman SM. 1999. A modified method for the display of 3′-end restriction fragments of cDNAs: Molecular profiling of gene expression in neutrophils. Methods Enzymol 303:272–297.

Teferedegne B, Green MR, Guo Z, Boss JM. 2006. Mechanism of action of a distal NF-kappaB-dependent enhancer. Mol Cell Biol 26:5759–5770.

Tucker KA, Lilly MB, Heck L Jr., Rado TA. 1987. Characterization of a new human diploid myeloid leukemia cell line (PLB-985) with granulocytic and monocytic differentiating capacity. Blood 70:372–378.

Vane J. 1994. Towards a better aspirin. Nature 367:215–216.

Voo KS, Carlone DL, Jacobsen BM, Flodin A, Skalnik DG. 2000. Cloning of a mammalian transcriptional activator that binds unmethylated CpG motifs and shares a CXXC domain with DNA methyltransferase, human trithorax, and methyl-CpG binding domain protein 1. Mol Cell Biol 20:2108–2121.

Yin MJ, Yamamoto Y, Gaynor RB. 1998. The anti-inflammatory agents aspirin and salicylate inhibit the activity of I(kappa)B kinase-beta. Nature 396:77–80.

SUPPORTING INFORMATION

Additional Supporting Information may be found in the online version of this article at the publisher's web-site.